SUPPLEMENTAL FIGURES:

Figure S1

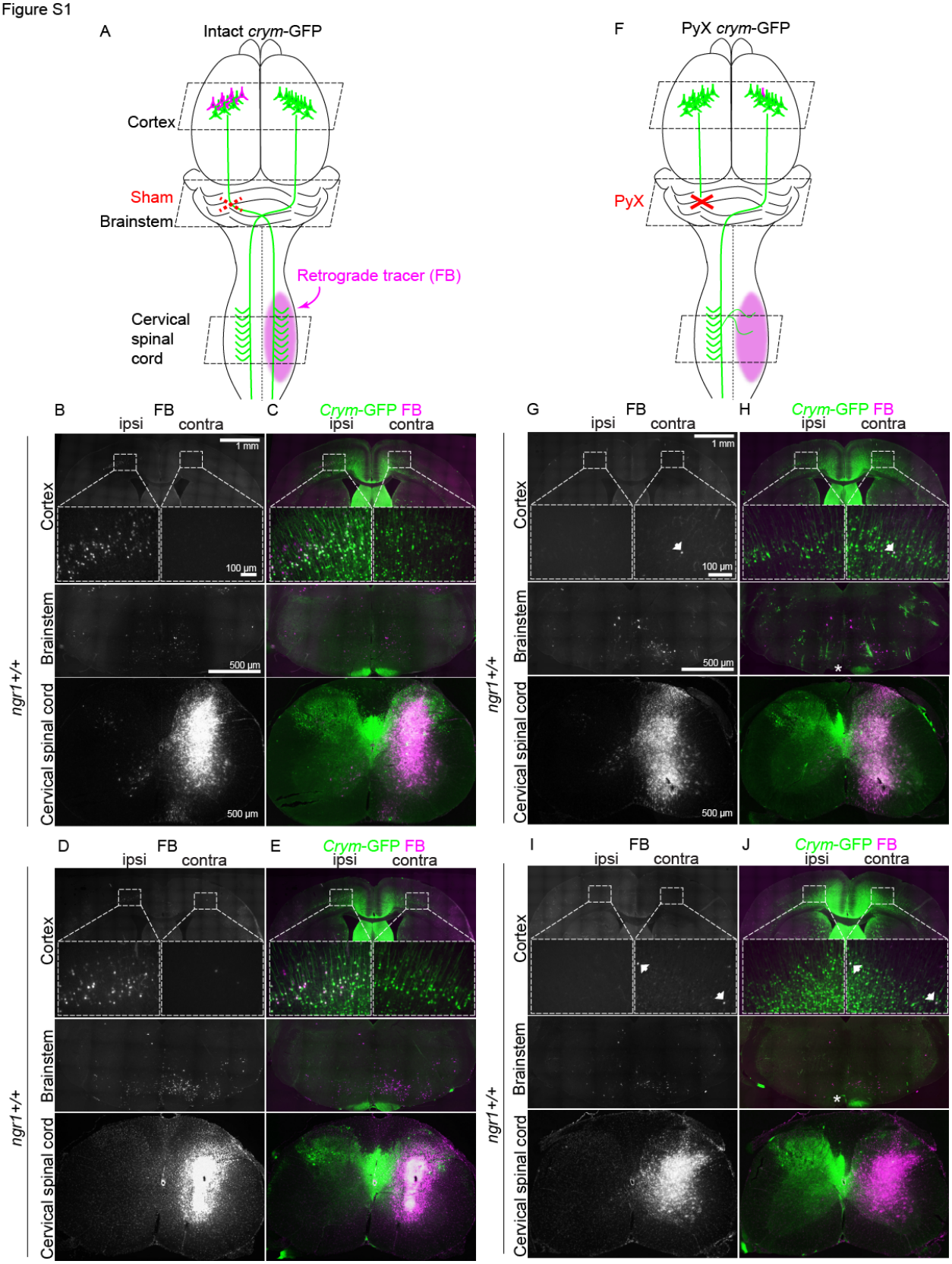

Figure S1 (related to Figure 1). Spinal retrograde labeling of CSMNs in *ngr1*$^{+/+}$ and *ngr1*$^{-/-}$ *crym*-GFP mice after sham and PyX lesion. Schematic (A) illustrate retrograde CSMN labeling via contralateral intraspinal infusion of Fast blue (FB, magenta) into the cervical enlargement of *ngr1*$^{+/+}$ (B-C) and *ngr1*$^{-/-}$ *crym*-GFP mice (D-E) after sham lesion (stippled red X, A). FB labeling in cortex is almost entirely ipsilateral to the sham lesion with scarce FB+ cells in contralateral cortex (B**,** D and insets). FB co-localizes with GFP+ CSMNs in *crym*-GFP mice (C**,** E and insets). Bilateral accumulation of FB in brainstem somata of crossed reticulospinal tract axons reveals fidelity of FB transport between genotypes (B, D). Integrity of the left CST is confirmed by *crym*-GFP+ axons observed bilaterally in the medullary pyramids (C, E). Spinal infusion of FB diffuses in the dorso-ventral plane, but remains unilateral after sham lesion and is taken up by *crym*-GFP+ CST axons (C, E). (F) illustrates retrograde CSMN labeling in *ngr1*$^{+/+}$ (G-H) and *ngr1*$^{-/-}$ (I-J) mice after PyX (red X, F). FB labeling in cortex (G-J) specifically labels CSMNs that have crossed the midline into the denervated spinal cord. There are no cells in cortex ipsilateral to PyX as a result of a complete lesion (G, I and insets). FB labels sprouting cells (arrows) in contralateral cortex with more cells labeled in *ngr1*$^{-/-}$ mice due to more spinal CST sprouting in these mice (G, I and insets). FB co-localizes with GFP+ CSMNs in *crym*-GFP mice (H, J and insets). The absence of *crym*-GFP in the left medullary pyramid confirms complete unilateral ablation of the CST (H, J asterisk). Scale bars = 100 and 500 μm.

Figure S2

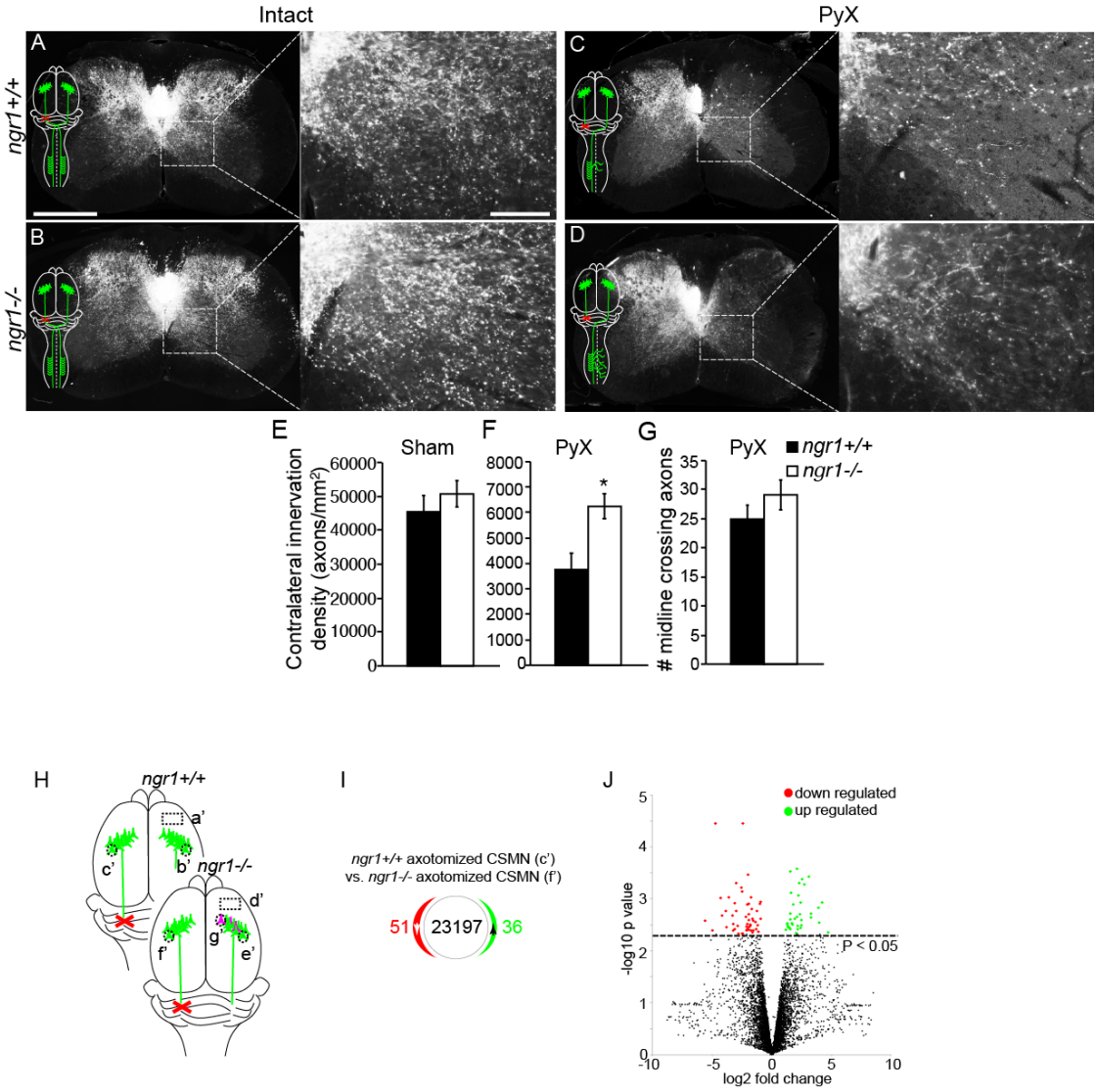

Figure S2 (related to Figure 2). *Crym*-GFP labeling of the CST reveals terminal sprouting in *ngr1*$^{-/-}$ mice and facilitates identification of discrete populations of CSMNs for LCM. Inset schematics (A-D) show lesion status for *crym*-GFP mice that underwent sham (stippled red X) or PyX (red X). *Crym*-GFP *ngr1*$^{+/+}$ (A) and *ngr1*$^{-/-}$ (C) mice show robust bilateral intrinsic labeling of the CST after sham lesion. Densitometric analysis of contralateral CST innervation was invariant between genotypes (E) after sham lesion. However, while sprouting of intact *crym*-GFP+ CST axons is seen in the contralateral (denervated) ventral horn in *ngr1*$^{+/+}$ mice (C, and inset), significantly more CST sprouting was seen in *ngr1*$^{-/-}$ mice (D, and inset, F, *P=0.04, student's t-test) after PyX. No significant difference was detected in the number of CST axons crossing the midline between genotypes, suggesting that the increase in CST density was due to sprouting of CST arbors in the denervated ventral horn (G).

Gene expression profiles were compared between axotomized CSMN samples from *ngr1*$^{+/+}$ and *ngr1*$^{-/-}$ mice 4 weeks after PyX (Schematic H, c' vs. f'). Only 51 genes were down regulated and 36 up regulated (I, 23,197 genes remained unchanged) in CSMN samples from *ngr1*$^{-/-}$ compared to *ngr1*$^{+/+}$ mice. Volcano plot (J) shows all profiled genes (green = up regulated, red = down regulated).

Figure S3

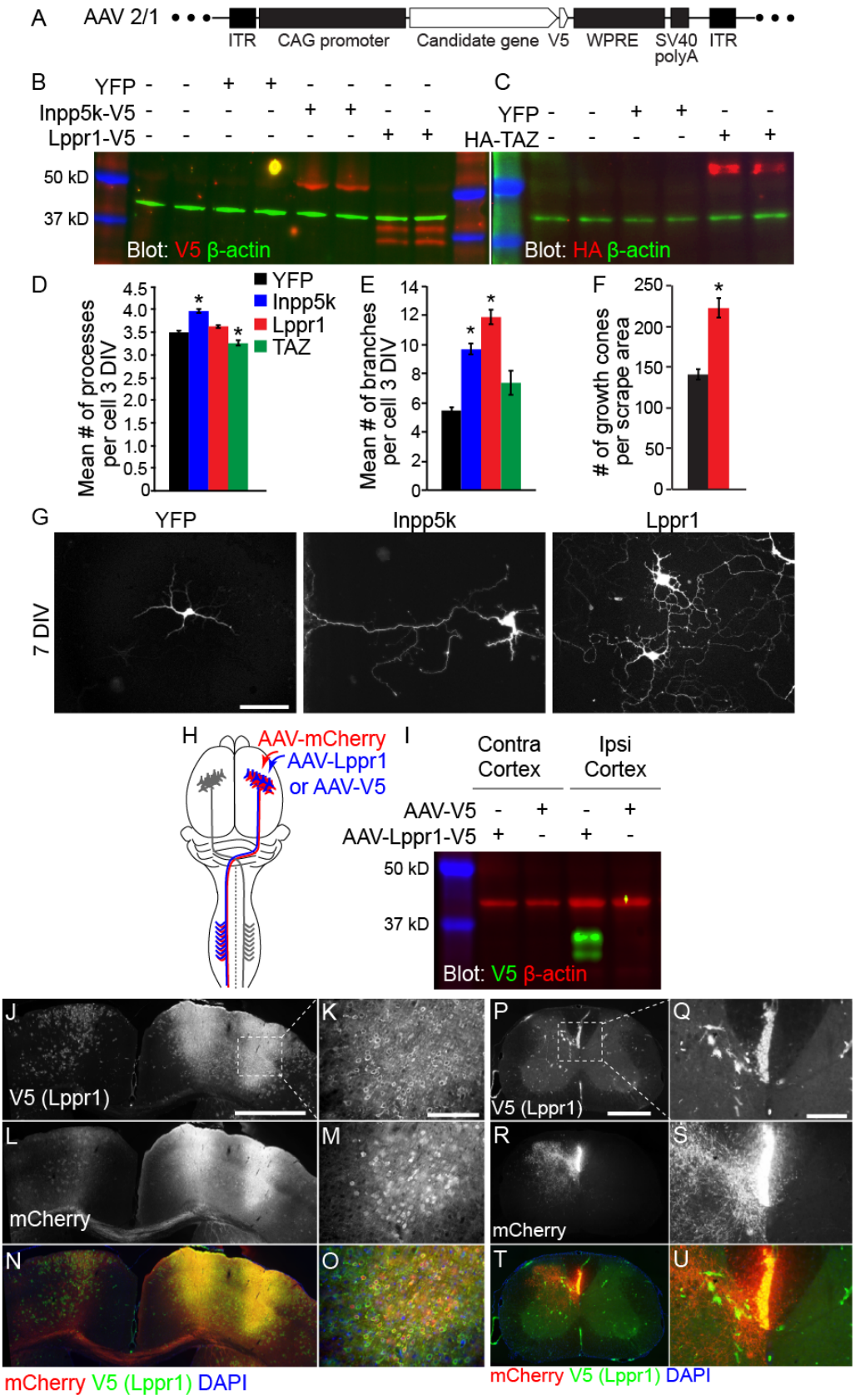
A
AAV 2/1
ITR
CAG promoter
Candidate gene
V5
WPRE
SV40 polyA
ITR
B
YFP
Inpp5k-V5
Lppr1-V5
50 kD
37 kD
Blot: V5 β-actin
C
YFP
HA-TAZ
Blot: HA β-actin
D
Mean # of processes per cell 3 DIV
YFP
Inpp5k
Lppr1
TAZ
E
Mean # of branches per cell 3 DIV
F
# of growth cones per scrape area
G
YFP
Inpp5k
Lppr1
7 DIV
H
AAV-mCherry
AAV-Lppr1
or AAV-V5
I
Contra Cortex
Ipsi Cortex
AAV-V5
AAV-Lppr1-V5
50 kD
37 kD
Blot: V5 β-actin
J
V5 (Lppr1)
K
L
mCherry
M
N
O
mCherry V5 (Lppr1) DAPI
P
V5 (Lppr1)
Q
R
mCherry
S
T
U
mCherry V5 (Lppr1) DAPI

Figure S3 (related to Figure 4). *In vitro* and *in vivo* validation of top candidate genes. Custom AAV 2/1 viruses were synthesized to overexpress candidate genes *in vitro* and *in vivo* under a CAG promoter (A). Dissociated cortical neurons were electroporated with plasmid AAV vectors and cultured for 7 DIV. Western blotting of RIPA extracted cell lysates revealed INPP5K and LPPR1 overexpression via detection of the V5 C-terminal tag (B) and TAZ overexpression by staining for the HA (human influenza hemagglutinin) N-terminal tag (C). LPPR1 runs as a ~35 kDa doublet as previously described (Sigal et al., 2007, Velmans et al., 2013). Additional outgrowth metrics were measured after acute transfection of E17 cortical neurons after 3 DIV. The mean number of processes was significantly increased in neurons expressing Inpp5k (D, *P<0.0001, one-way ANOVA followed by Dunnett's *post hoc* test), and significantly decreased in neurons expressing TAZ (*P<0.005, one-way ANOVA followed by Dunnett's *post hoc* test). Overexpression of INPP5K and LPPR1 results in a significant increase in the number of neurite branches per cell (E, *P<0.0001, one-way ANOVA followed by Dunnett's *post hoc* test). Data for processes and branches are presented as the mean ± SEM, averaged over 4 sites per well from 3 biological replicates, n=62-69 wells per condition. In the cortical neuron scrape assay, overexpression of LPPR1 resulted in a significant increase in the number of growth cones normalized to total scrape area (F, *P<0.0001, student's t-test). Qualitative analysis of dissociated cortical neurons 7 DIV shows neurons overexpressing YFP have smaller neurites with fewer branches than neurons overexpressing INPP5K or LPPR1 (G).
Schematic (H) shows cortical transduction of CSMNs with either AAV-*Lppr1*-V5 or AAV-*V5* control (blue) and AAV-*mCherry* (red) in adult wild type mice. Two weeks post-infusion, motor cortex contra and ipsilateral to the infusion was dissected and RIPA-extracted lysates prepared for immunoblotting. Antibodies to V5 detected a doublet in ipsi cortex at ~35 kD consistent with the expected molecular weight of LPPR1 (I). Immunostaining of transverse sections of cortex (J-O) and cervical spinal cord (P-U) revealed a high co-transduction of V5 and mCherry. V5 staining revealed a non-nuclear expression pattern of LPPR1 in cortical neurons (J, and inset K) and fasciculated CST axons in the spinal cord (P, inset Q). mCherry co-localizes with the V5 transduced cortical neurons (N-O) and fasciculated CST axons in the spinal cord (T-U). mCherry efficiently labels CST terminals throughout spinal grey matter and hence was used for CST axon densitometric quantification owing to its near 1:1 overlap with LPPR1 transduced CSMNs.

Figure S4

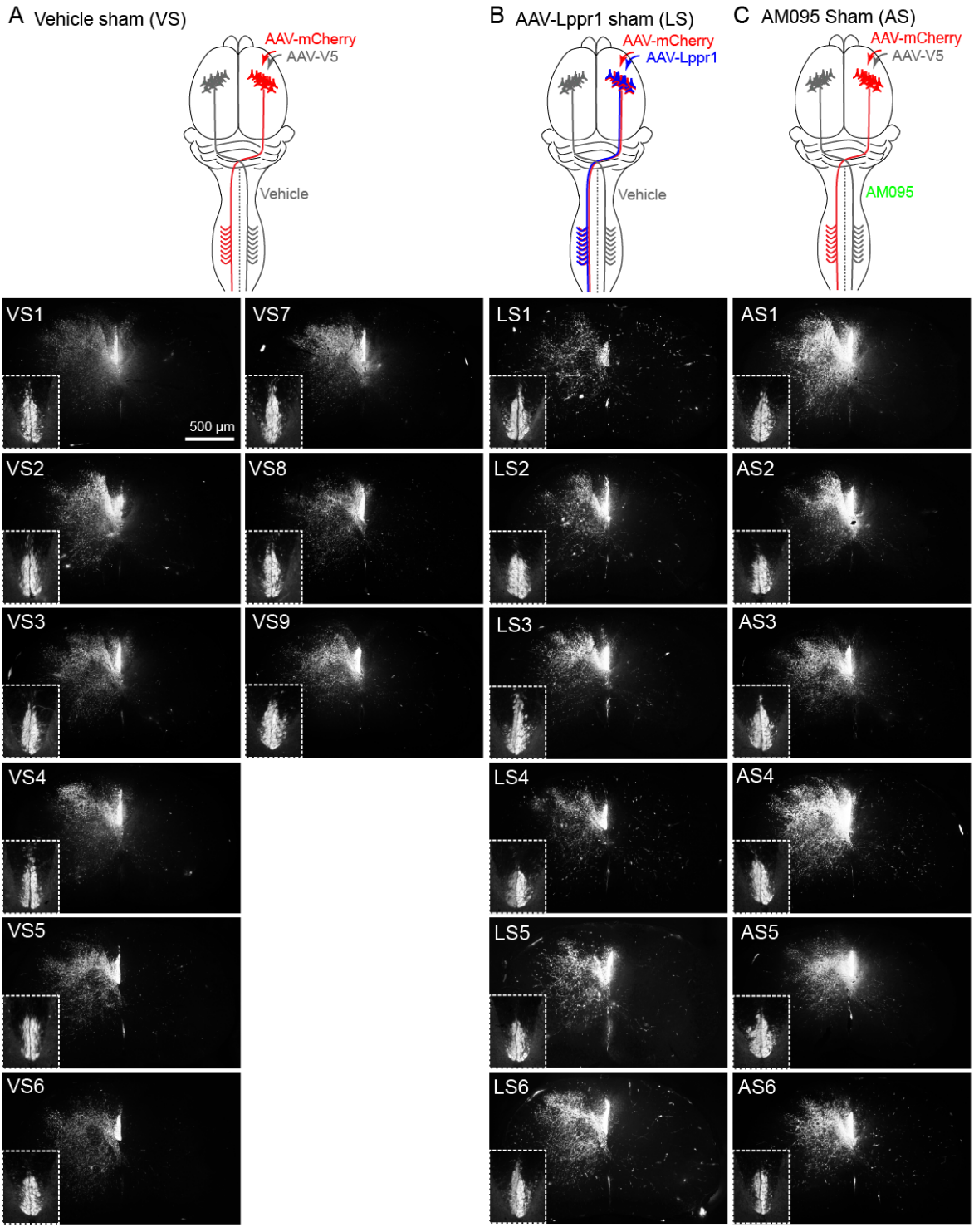

Figure S4 (related to Figure 6). AAV-*Lppr1* and AM095 treated mice show an increase in CST innervation of the ventral horn after sham lesion. mCherry+ axon labeling of the intact CST from every sham lesioned animal included in anatomical analysis is shown for vehicle (A, VS, n=9), AAV-*Lppr1* (B, LS, n=6), and AM095 (C, AS, n=6) groups. Insets in each transverse spinal cord section show bilateral PKCgamma staining in the ventral dorsal columns confirming sham lesion.

Figure S5

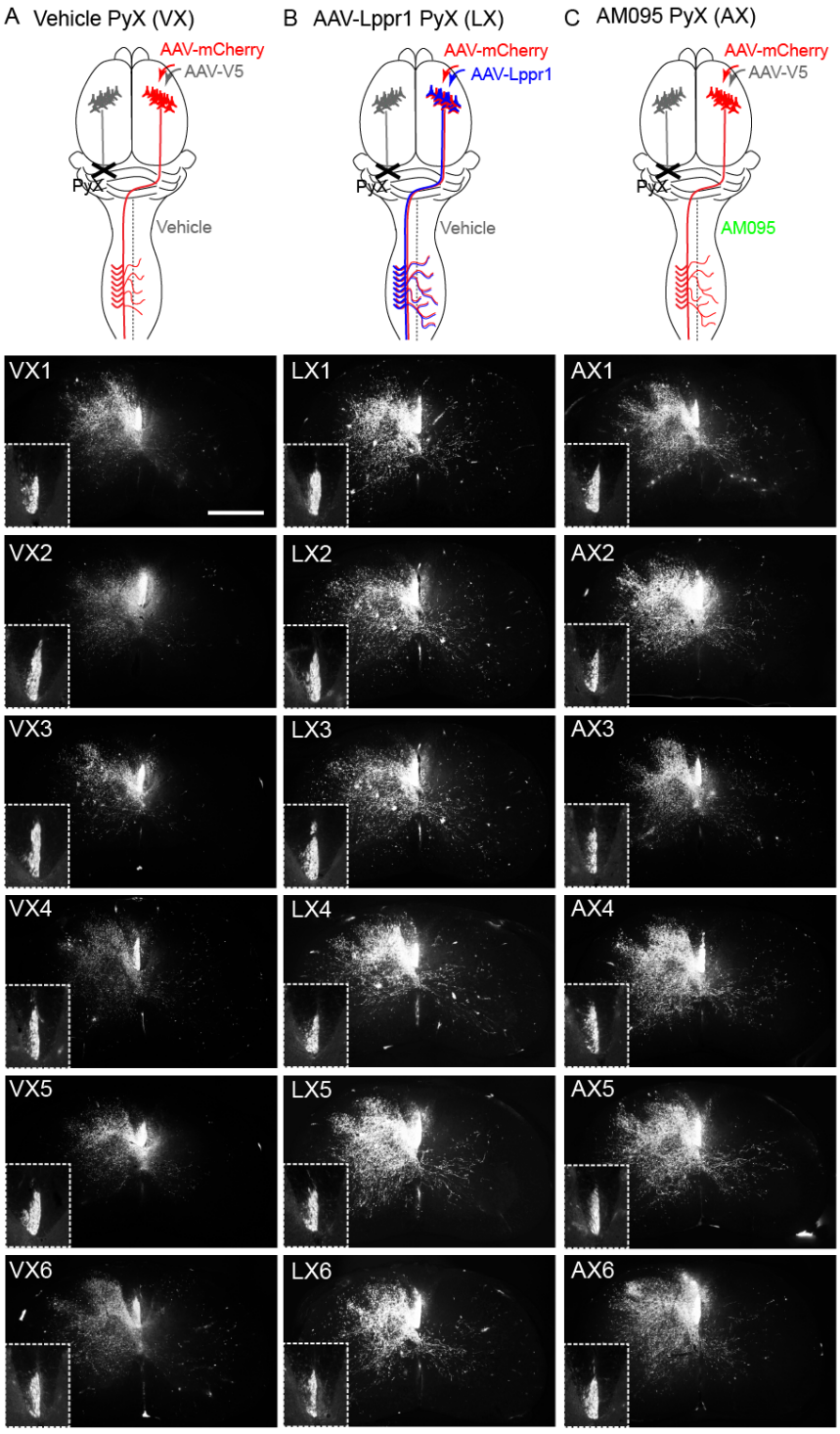

Figure S5 (related to Figure 6). AAV-*Lppr1* and AM095 treated mice show an increase in CST innervation of the ventral horn after PyX. mCherry+ axon labeling of the intact CST from every PyX animal included in anatomical analysis is shown for vehicle (**a**, VX, n=10), AAV-*Lppr1* (**b**, LX, n=15), and AM095 (**c**, AX, n=9) groups. Insets in each transverse spinal cord section show unilateral PKCgamma staining in the ventral dorsal columns confirming PyX lesion.

Figure S6

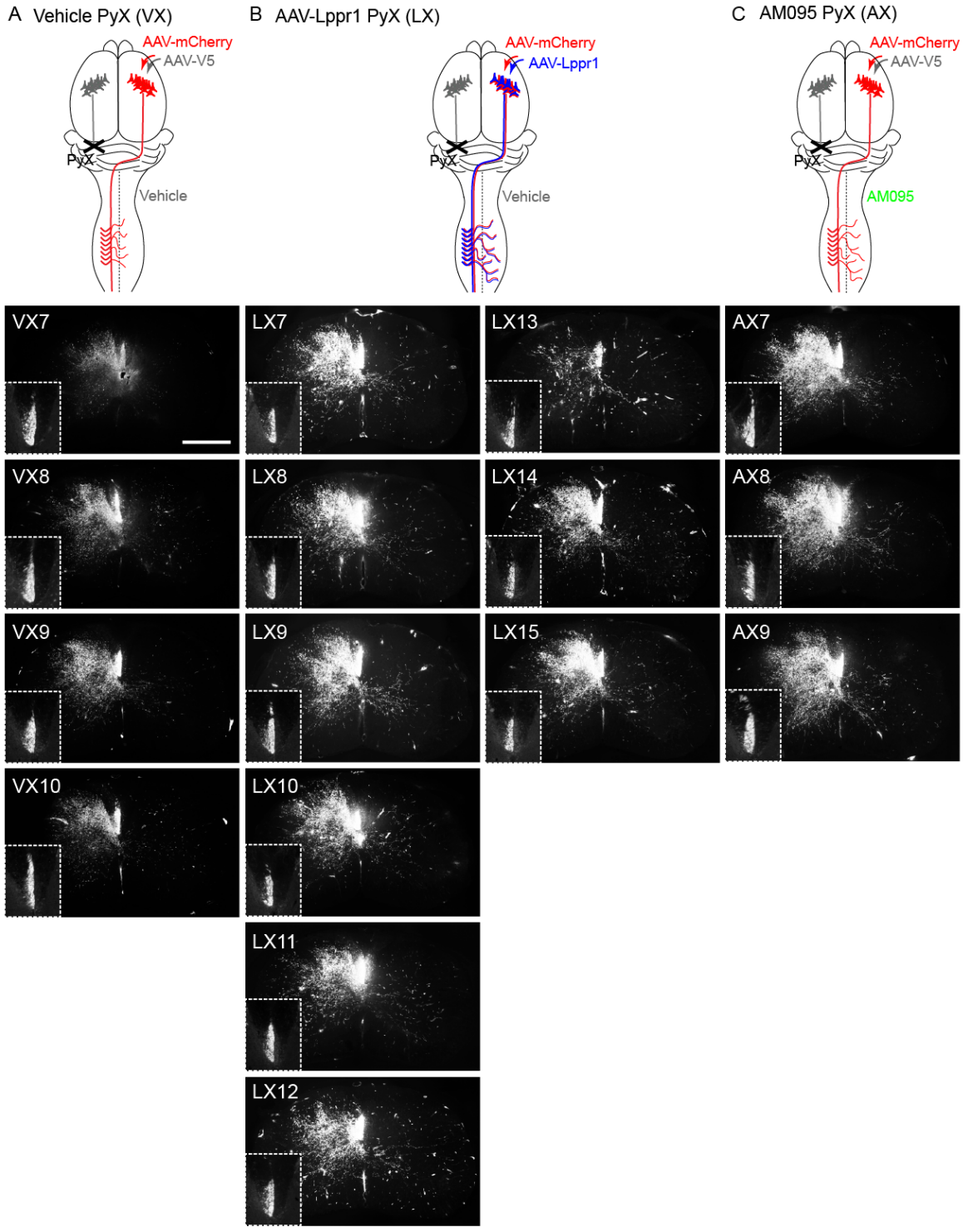

Figure S6 (related to Figure 6). AAV-*Lppr1* and AM095 treated mice show an increase in CST innervation of the ventral horn after PyX. mCherry+ axon labeling of the intact CST from every PyX animal (continued from Figure S5) included in anatomical analysis is shown for vehicle (**a**, VX, n=10), AAV-*Lppr1* (**b**, LX, n=15), and AM095 (**c**, AX, n=9) groups. Insets in each transverse spinal cord section show unilateral PKCgamma staining in the ventral dorsal columns confirming PyX lesion.

Figure S7

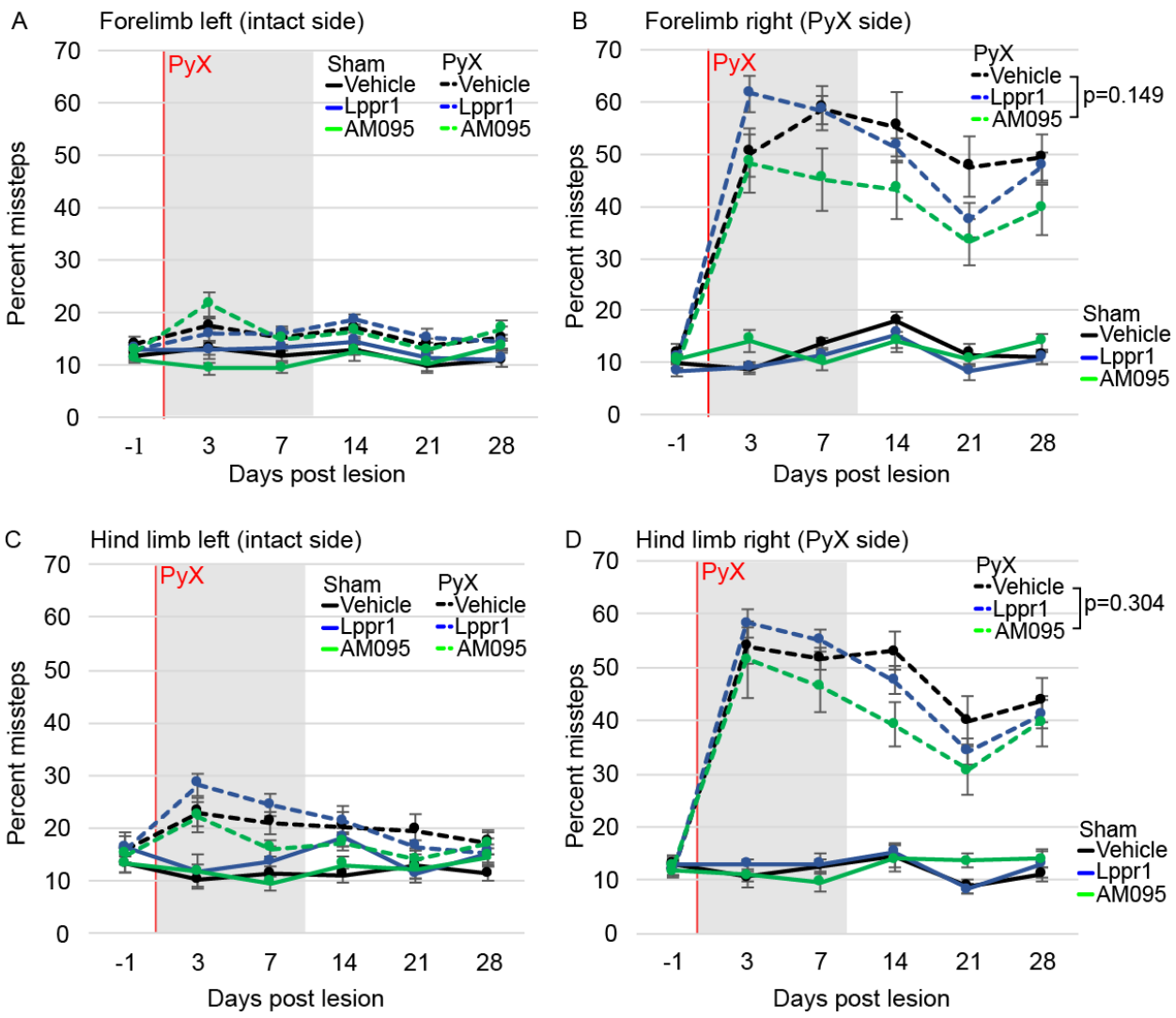

Figure S7 (related to Figure 6). Performance of each limb after PyX or sham lesion.
Grid walking analysis showed that sham lesioned mice did not show a significant difference in fine motor function between treated groups (vehicle = black, LPPR1-treated = blue, AM095-treated = green solid lines) in forelimbs (A, B) or hind limbs (C, D) on the intact (A, C) or denervated side (B, D) during the experimental period. Mice that underwent PyX lesion from all treatment groups (vehicle = black, LPPR1-treated = blue, AM095-treated = green stippled lines) also did not show a significant impairment in skilled motor function on the intact side throughout the experimental period (A, C). Mice from all treatment groups that PyX showed a significant impairment in grid walking performance in both the forelimb (B) and hind limb (D) on the denervated side. AM095 treated mice showed a trend to toward significant recovery in forelimb (B, P = 0.149, one-way ANOVA with repeated measures) and hind limb (D, P = 0.304, one-way ANOVA with repeated measures) performance over the experimental period.

Table S1

Total number of individual cell collected (n=6)	16, 612
Average number of cells collected/ animal	923
Average number of cells collected per cortex	460
Average area *crym*-GFP cells collected per cortex	750, 302 µm
Average area of non-GFP cells collected per cortex	689, 197 µm

Table S1 (related to Figure 2). LCM was performed on cortical sections from *crym*-GFP $ngr1^{+/+}$ (n=6) and $ngr1^{-/-}$ (n=6) mice 2 weeks post contralateral cervical spinal infusion with FB and 4 weeks after PyX. Table summarizes the total number of individual CSMNs collected, the cumulative area of those cells, and the area of non-CSMN cortex collected as control.

Table S2

	$ngr1^{+/+}$ intact non-CSMNs	$ngr1^{+/+}$ intact quiescent CSMNs	$ngr1^{+/+}$ axotomized CSMNs	$ngr1^{-/-}$ intact non-CSMNs	$ngr1^{-/-}$ intact quiescent CSMNs	$ngr1^{-/-}$ axotomized CSMNs	$ngr1^{-/-}$ intact sprouting CSMNs
Total reads	55887203	47457092	60607706	56317112	45588494	59740508	42001406
unique (% av., n=3)	91.3	87.3	86.1	91.2	85.5	87.9	72.3
Total in genes (% av., n=3)	70.6	64.4	62.1	71.1	64.8	68.1	53

Table S2 (related to Figure 2). LCM samples were pooled from two animals at random to obtain 3 replicates per condition from 6 animals per genotype. RNAseq was performed on LCM samples for a minimum of 40 million reads per sample. Table displays average number of reads per condition (n=3 samples per condition), the percent of unique reads, and the percent of total reads in genes.

Table S3

Top 50 upregulated *ngr1*$^{+/+}$			Top 50 down regulated *ngr1*$^{+/+}$		
Gene	Log2 fold Δ	P value	Gene	Log2 fold Δ	P value
Foxp2	5.71	0.0012	*Pld5*	-6.06	0.0165
Syt6	5.20	0.0012	*Gpr88*	-5.83	0.0012
Ipw	5.20	0.0022	*Plxnd1*	-5.30	0.0012
Col6a1	5.18	0.0022	*Myom3*	-5.06	0.0413
Sebox	5.17	0.0072	*Prelp*	-5.05	0.0294
Col5a1	4.94	0.0358	*Tmem215*	-5.04	0.0066
Rai14	4.47	0.0079	*Etnk2*	-4.94	0.0358
Col23a1	4.30	0.0212	*Pctp*	-4.65	0.0460
Ryr3	4.02	0.0045	*Gcnt1*	-4.39	0.0453
Lsp1	3.98	0.0022	*Coch*	-4.16	0.0059
Figf	3.93	0.0466	*Ptgfrn*	-4.14	0.0150
Nxph3	3.91	0.0030	*Igfbp2*	-4.14	0.0012
Sla	3.48	0.0012	*Hmgcs2*	-4.10	0.0263
Rprm	3.45	0.0012	*Ddit4l*	-4.05	0.0012
4930447C04Rik	3.40	0.0212	*Ormdl1*	-4.05	0.0038
Slc44a5	3.39	0.0250	*LOC626082*	-4.01	0.0417
Gm12824	3.30	0.0287	*Klhdc8a*	-3.82	0.0059
Obscn	3.30	0.0202	*Sult1a1*	-3.81	0.0400
Hs3st4	3.25	0.0012	*Scn7a*	-3.80	0.0390
4932411L15	3.23	0.0012	*Otof*	-3.74	0.0267
Drd1a	3.20	0.0130	*Ttpa*	-3.71	0.0400
Sema3f	3.18	0.0279	*Gpr153*	-3.63	0.0045
Pcsk5	3.16	0.0310	*Fzd6*	-3.50	0.0347
Crym	3.15	0.0012	*Calb1*	-3.50	0.0012
A330076H08Rik	3.09	0.0012	*Ppp1r3g*	-3.44	0.0066
Sema5b	3.09	0.0072	*Car8*	-3.38	0.0038
Syt10	3.07	0.0202	*Acsf2*	-3.38	0.0108
Prss22	3.06	0.0306	*Pvrl3*	-3.35	0.0012
Sema5a	3.06	0.0012	*Slc24a6*	-3.30	0.0463
Lin28b	3.04	0.0302	*Synpr*	-3.29	0.0012
Grik3	3.02	0.0012	*Dbx2*	-3.23	0.0052
Oprk1	3.00	0.0130	*Tnnc1*	-3.23	0.0329
Drd5	3.00	0.0434	*Nupr1*	-3.18	0.0189
Zfpm2	2.99	0.0012	*Bhlhe22*	-3.17	0.0012
Col12a1	2.93	0.0202	*Smoc2*	-3.13	0.0022
Rgs9	2.92	0.0150	*Apln*	-3.13	0.0012
F830016B08Rik	2.91	0.0329	*Pdzrn3*	-3.13	0.0012
Spsb1	2.91	0.0012	*Ndp*	-3.10	0.0263
Sulf1	2.89	0.0030	*Zhx2*	-3.09	0.0202
Nfe2l3	2.85	0.0410	*Hsd11b1*	-3.08	0.0453
Prss35	2.84	0.0119	*Ocln*	-3.07	0.0140
Odz3	2.81	0.0012	*Mxra7*	-2.98	0.0052
Pdlim1	2.76	0.0108	*Chrdl1*	-2.96	0.0045
Ptpru	2.74	0.0012	*Fam163a*	-2.96	0.0294
Meg3	2.73	0.0012	*Gldc*	-2.96	0.0022
Kcnq1ot1	2.69	0.0012	*Swap70*	-2.95	0.0413
Arhgap25	2.66	0.0072	*Aldh1a1*	-2.94	0.0012
Sdk2	2.66	0.0340	*Crhr1*	-2.94	0.0160
Gdpd5	2.65	0.0022	*Stard8*	-2.92	0.0012
Snhg11	2.65	0.0012	*Tmem176a*	-2.91	0.0372
Enriched in neurons vs. astrocytes Enriched in CSMNs at P7			Enriched in astrocytes vs. neurons		

Top 50 upregulated *ngr1*$^{-/-}$			Top 50 down regulated *ngr1*$^{-/-}$		
Gene	Log2 fold Δ	P value	Gene	Log2 fold Δ	P value
Syt6	5.42	0.0022	*Tifa*	-5.22	0.0160
Fam184b	5.18	0.0396	*Cux2*	-5.15	0.0085
Lsp1	4.28	0.0102	*Pdzrn3*	-4.83	0.0059
Ntsr1	4.27	0.0108	*Aass*	-4.71	0.0383
Col6a1	4.03	0.0140	*Irgm2*	-4.32	0.0390
Foxp2	4.03	0.0012	*Fam163a*	-4.24	0.0091
Foxo6	3.52	0.0446	*Phka1*	-4.19	0.0160
Pcsk5	3.47	0.0091	*Prrg1*	-4.09	0.0271
Ramp3	3.46	0.0012	*Tmie*	-4.06	0.0351
Grp	3.42	0.0012	*Coch*	-4.04	0.0066
Zfp229	3.35	0.0460	*Plxnd1*	-3.75	0.0012
Rprm	3.32	0.0012	*Prkg2*	-3.72	0.0135
Sla	3.19	0.0012	*Aldh1a1*	-3.60	0.0012
Glra2	3.17	0.0038	*Ttpa*	-3.58	0.0446
Zfpm2	3.16	0.0022	*Suclg2*	-3.57	0.0012
Rai14	3.15	0.0393	*Kcnh5*	-3.57	0.0012
Sema5a	3.04	0.0012	*Aldh1l1*	-3.47	0.0012
Gm12824	3.04	0.0410	*Prom1*	-3.45	0.0059
Nfe2l3	3.04	0.0233	*Stom*	-3.45	0.0302
D930016D06Rik	3.01	0.0066	*1700084C01Rik*	-3.35	0.0443
Col23a1	2.99	0.0336	*Rfx4*	-3.34	0.0473
Crym	2.88	0.0012	*Kcnj16*	-3.34	0.0030
Ipw	2.83	0.0170	*Nde1*	-3.27	0.0160
Gm1337	2.81	0.0085	*Apln*	-3.25	0.0030
Klhl25	2.81	0.0271	*Tcap*	-3.24	0.0165
Ldb3	2.80	0.0423	*Gldc*	-3.20	0.0012
Nxph3	2.79	0.0012	*Klhdc8a*	-3.19	0.0012
Btg2	2.76	0.0255	*Cpne9*	-3.16	0.0012
Npr3	2.72	0.0242	*Atp13a5*	-3.14	0.0495
Rnf152	2.70	0.0012	*Gramd3*	-3.11	0.0066
Fancd2	2.69	0.0354	*Tek*	-3.09	0.0242
Prss35	2.67	0.0179	*Phactr2*	-3.09	0.0038
Grik3	2.66	0.0012	*Gja1*	-3.08	0.0012
Sulf1	2.60	0.0361	*Yes1*	-3.07	0.0160
Fgf10	2.59	0.0198	*Emx2*	-3.06	0.0045
Arhgap25	2.53	0.0072	*Amot*	-3.06	0.0045
Cdh13	2.50	0.0012	*Slc25a18*	-3.05	0.0012
Hs3st4	2.49	0.0012	*Bhlhe22*	-3.05	0.0012
Igfbp4	2.45	0.0012	*Prodh*	-3.04	0.0113
Dpysl5	2.34	0.0271	*Car8*	-3.02	0.0012
A330076H08Rik	2.31	0.0456	*Gpr153*	-2.98	0.0022
Pdzrn4	2.29	0.0096	*Exph5*	-2.96	0.0012
Aldh1b1	2.29	0.0255	*Fgf1*	-2.95	0.0012
1700019D03Rik	2.26	0.0170	*B230120H23Rik*	-2.93	0.0287
Tle4	2.26	0.0012	*Hapln1*	-2.93	0.0052
Igsf21	2.21	0.0012	*Klhdc7a*	-2.89	0.0463
Serinc2	2.18	0.0275	*Dio2*	-2.89	0.0012
Drd1a	2.16	0.0279	*Vcam1*	-2.87	0.0255
Grik4	2.14	0.0460	*Tgfb1*	-2.85	0.0463
Tmsb10	2.14	0.0012	*Itih5*	-2.83	0.0052
Enriched in neurons vs. astrocytes Enriched in CSMNs at P7			Enriched in astrocytes vs. neurons		

Table S3 (related to Figure 2). *Crym*-GFP samples from *ngr1*$^{+/+}$ and *ngr1*$^{-/-}$ mice are enriched for known neuronal and CSMN genes. Gene expression profiles were compared between non-CSMNs and intact CSMNs 4 weeks after PyX in *ngr1*$^{+/+}$ mice. Table lists the top 50 SDE genes up regulated (neuronal genes listed in blue, CSMN genes listed in green) (Arlotta et al., 2005) (Zhang et al., 2014) and top 50 genes down regulated (astrocyte genes listed in red) in intact CSMN samples vs. non-CSMN samples in *ngr1*$^{+/+}$ mice and *ngr1*$^{-/-}$ mice. SDE genes are listed with log2 fold change and FDR corrected p-values.

Table S4

Gene	Log2 FΔ	P value
***ngr1*$^{+/+}$ vs. *ngr1*$^{-/-}$ non-CSMN**		
Cyp26b1	1.91	0.0096
Cotl1	1.45	0.0347
Slc24a3	1.36	0.0119
Spon1	1.31	0.0358
Cadm3	1.22	0.0189
Sulf2	1.22	0.0450
Hs3st2	1.22	0.0386
Hrh3	1.20	0.0207
Ppp1r16b	1.20	0.0462
Fzd3	-1.06	0.0420
Kitl	-1.13	0.0259
Wipf3	-1.15	0.0407
Kctd1	-1.22	0.0403
Vip	-1.36	0.0267
Matn2	-1.37	0.0446
Gucy1a3	-1.49	0.0022
Rasgrf2	-1.66	0.0012
Zfp930	-1.74	0.0358
Ddx3y	-1.88	0.0298
Calb1	-2.01	0.0012
Gm1337	-2.54	0.0202
Fcho1	-2.58	0.0012
E130309F12Rik	-2.73	0.0079
Fam184b	-4.62	0.0492
Rtn4r	-5.13	0.0012
***ngr1*$^{+/+}$ vs. *ngr1*$^{-/-}$ quiescent CSMN**		
St8sia2	4.39	0.0450
Esyt3	3.61	0.0434
Usp43	3.56	0.0321
Mal	-1.25	0.0390
A330076H08Rik	-1.27	0.0495
Slc35a5	-1.52	0.0250
Fcho2	-1.57	0.0310
Mid2	-1.60	0.0332
Trim59	-1.60	0.0423
Ugt8a	-1.62	0.0267
Il33	-1.69	0.0306
Fastkd2	-1.70	0.0469
Oprk1	-1.73	0.0460
Slc5a5	-1.91	0.0102
Traf6	-1.97	0.0466
Serpina3n	-2.06	0.0102
Zfp790	-2.06	0.0372
Ncapg2	-2.25	0.0396
Zfp182	-2.36	0.0329
Uty	-2.47	0.0376
Ddx3y	-2.47	0.0066
Prrg1	-4.02	0.0358
Lin28b	-4.17	0.0179
Stra6	-4.28	0.0298
Rtn4r	-5.78	0.0038

Gene	Log2 FΔ	P value
***ngr1*$^{+/+}$ intact vs. axotomized CSMN**		
Prelp	4.48	0.0054
Phf16	3.99	0.0036
Hic1	3.80	0.0025
Mocs1	3.71	0.0014
AA415398	3.57	0.0020
Nid1	3.38	0.0033
Cyp4f16	3.36	0.0057
Gpr4	3.11	0.0040
Prkcd	2.98	0.0046
Zhx2	2.90	0.0027
Zfp174	2.62	0.0057
Fam114a1	2.54	0.0042
Plekhh3	2.52	0.0029
Crhr1	2.51	0.0038
Ccdc88c	2.17	0.0016
Atad2	2.11	0.0034
Scaf4	2.07	0.0013
Elf2	1.99	0.0037
Ptk7	1.92	0.0023
Ndor1	1.84	0.0036
Klhl28	1.84	0.0020
Kcnj12	1.80	0.0015
Cbl	1.63	0.0030
Ipo7	1.52	0.0009
Uevld	1.41	0.0044
Asb6	1.38	0.0033
Zdbf2	1.32	0.0019
Papolg	-1.60	0.0045
Zfp598	-1.72	0.0048
Tmem43	-1.80	0.0021
Ppp1r26	-1.95	0.0041
Rnf138	-1.98	0.0007
Sec14l2	-2.33	0.0054
Pcdh11x	-2.35	0.0048
Arhgef10	-2.45	0.0029
Nif3l1	-2.50	0.0018
Engase	-3.08	0.0033
Tgfa	-3.25	0.0032
Gprc5c	-3.42	0.0040
Trmt2b	-3.89	0.0023
Nipal4	-4.20	0.0038
H6pd	-4.72	0.0033
***ngr1*$^{-/-}$ intact vs. axotomized CSMN**		
Nfatc1	3.91	0.0035
Zfhx4	2.92	0.0043
Zfp182	2.22	0.0048
Bhlhe22	1.89	0.0038
Eef1a2	1.58	0.0010
Ugt8a	1.57	0.0037
Fcho2	1.56	0.0026
Snapc1	1.41	0.0034
Hdac9	1.31	0.0035
Dmxl1	1.27	0.0027
Stxbp6	1.14	0.0035
Rps29	-1.06	0.0054
Lrrc17	-1.40	0.0007
2700007P21Rik	-1.45	0.0051
Pde3b	-2.09	0.0056
Zfp112	-2.17	0.0054
Wbscr16	-2.41	0.0019
Ttc23	-3.99	0.0043
Zfp229	-5.86	0.0030

Gene	Log2 FΔ	P value
***ngr1*$^{+/+}$ vs. *ngr1*$^{-/-}$ axotomized CSMN**		
Col11a2	4.66	0.0055
Trmt2b	4.15	0.0015
Otof	3.95	0.0036
Gprc5c	3.87	0.0019
Podxl	3.26	0.0029
Engase	3.26	0.0024
C330018D20Rik	3.05	0.0005
Nif3l1	2.69	0.0007
Fbxl18	2.52	0.0006
Sec14l2	2.45	0.0040
Zfp282	2.43	0.0032
Pcdh11x	2.40	0.0045
Abi3bp	2.39	0.0015
Lpl	2.30	0.0025
Fbrs	2.23	0.0007
Ltbp4	2.18	0.0011
Scrib	2.15	0.0042
Zswim4	2.14	0.0047
Ampd2	2.04	0.0004
Vip	2.03	0.0028
Gpr75	2.00	0.0056
Itga4	1.90	0.0030
2310047M10Rik	1.77	0.0017
Fbxw8	1.66	0.0039
Ctbp2	1.66	0.0037
Neurl4	1.59	0.0010
Prmt7	1.53	0.0024
Cpne4	1.52	0.0032
Synpr	1.50	0.0004
Cep68	1.49	0.0048
Uba6	1.41	0.0045
Vipar	1.34	0.0042
Ifrd1	1.31	0.0044
Nbl1	1.27	0.0037
D730040F13Rik	1.24	0.0039
Plekha1	1.12	0.0048

Gene	Log2 FΔ	P value
***ngr1*$^{+/+}$ vs. *ngr1*$^{-/-}$ axotomized CSMN**		
Malat1	-0.97	0.0015
Kcnq1ot1	-1.00	0.0031
Snhg11	-1.04	0.0016
Rock1	-1.19	0.0053
Krit1	-1.24	0.0040
Tbc1d9	-1.28	0.0022
Rpl7l1	-1.34	0.0048
Dhrs1	-1.43	0.0035
Erlin1	-1.60	0.0050
Rnpc3	-1.61	0.0033
Tril	-1.66	0.0055
D3Ertd751e	-1.67	0.0031
Fcho1	-1.72	0.0020
Ugdh	-1.75	0.0012
Gm7120	-1.80	0.0051
Ndor1	-1.81	0.0039
Ccdc88c	-1.84	0.0041
Tmem39b	-1.94	0.0043
BC024479	-1.95	0.0032
Ptk7	-1.99	0.0016
Pard3	-1.99	0.0025
Scfd2	-1.99	0.0049
Zfhx3	-2.04	0.0005
Cyr61	-2.09	0.0038
Unc5d	-2.09	0.0017
3110057O12Rik	-2.12	0.0048
Ifit2		
Fam176a	-2.15	0.0042
Hsf2	-2.24	0.0028
Slc5a5	-2.46	0.0001
Cpsf4	-2.49	0.0058
Skp2	-2.54	0.0058
Klhl1	-2.54	0.0010
Serpina3n	-2.56	0.0008
Mocs1	-2.84	0.0058
Gas2l3	-2.89	0.0042
Rarb	-3.00	0.0022
Uty	-3.05	0.0007
Zfp423	-3.16	0.0016
S1pr3	-3.17	0.0048
Gpr4	-3.26	0.0038
Car12	-3.30	0.0051
Hr	-3.32	0.0027
Pcsk6		
C1qtnf6	-3.83	0.0044
Npnt	-3.86	0.0022
Hus1	-4.21	0.0026
Slco2b1	-4.35	0.0013
Rtn4r	-4.77	0.0001
BC030476	-5.03	0.0051
Cav1	-5.64	0.0033

Table S4 (related to Figure 2). Minimal compensatory changes in cortical gene expression in intact non-CSMNs, intact CSMNs and axotomized CSMNs between *ngr1*$^{-/-}$ vs. *ngr1*$^{+/+}$ mice. Gene expression profiles were compared between control non-CSMNs from *ngr1*$^{+/+}$ and *ngr1*$^{-/-}$ mice 4 weeks after PyX. Table lists the 25 SDE genes (9 up regulated = green, 16 down regulated = red) along with corresponding log2 fold change and FDR corrected p-values. Only 25 (3 up regulated, 22 down regulated) genes were SDE between intact CSMNs from *ngr1*$^{+/+}$ and *ngr1*$^{-/-}$ mice 4 weeks after PyX. Notably *ngr1* (*Rtn4r*) is the most significantly down regulated gene between both comparisons.

Gene expression profiles were also compared between axotomized and intact CSMN samples from *ngr1*$^{+/+}$ mice 4 weeks after PyX. Table S4 lists the 42 SDE genes (27 up regulated = green, 15 down regulated = red). Only 19 (11 up regulated, 8 down regulated) genes were SDE between axotomized and intact CSMN samples from *ngr1*$^{-/-}$ mice 4 weeks after PyX.
Gene expression profiles were compared between axotomized CSMN samples from *ngr1*$^{+/+}$ and *ngr1*$^{-/-}$ mice 4 weeks after PyX. Only 36 SDE genes were up regulated (green), the 51 genes were down regulated (red).

SUPPLEMENTAL EXPERIMENTAL PROCEDURES

Surgery

Unilateral pyramidotomy (PyX)

To complete PyX, P56 adult male *ngr1*$^{+/+}$ *crym*-GFP (n=15) and *ngr1*$^{-/-}$ *crym*-GFP (n=15) mice were anesthetized with ketamine (100mg/kg) and xylazine (15mg/kg) and placed in a supine position, an incision was made to the left of the trachea, and blunt dissection exposed the occipital bone at the base of the skull. The occipital bone was removed on the left side of the basilar artery with blunt Dumont #2 forceps to expose the medullary pyramids. The dura mater was pierced with a 30-gauge needle and resected. The left pyramid was transected unilaterally with fine Dumont #5 forceps to a depth of 0.25 mm or exposed for sham lesion. No internal sutures were made and skin was closed with monofilament suture.

Intraspinal retrograde Fast Blue (FB) tracing

Two weeks after PyX, mice received contralateral Intraspinal injection of FB retrograde tracer to label sprouting neurons. To complete retrograde FB labeling of sprouting CSMNs, adult male *ngr1*$^{+/+}$ *crym*-GFP (n=15) and *ngr1*$^{-/-}$ (n=15) *crym*-GFP mice that had received PyX 14 days prior, and age-matched unlesioned adult male *crym*-GFP *ngr1*$^{+/+}$ (n=6) and *crym*-GFP *ngr1*$^{-/-}$ (n=9) mice were anesthetized with ketamine (100mg/kg) and xylazine (15mg/kg) and placed in a stereotaxic frame (Stoelting, USA). An incision was made over the cervical enlargement and the C5-C8 vertebrae revealed by blunt dissection of overlying muscle. A hemi-laminectomy was performed to expose the underlying C5-C8 spinal cord and a small incision was made in the dura mater. The tip of a pulled glass capillary tube attached to a Micro4 infusion device (World Precision Instruments, USA) was slowly inserted stereotaxically to a depth of 500 µm into the C5 level of the spinal cord and approximately 500 µm lateral from the midline. Thirty seconds after introduction of the capillary tube 75 nl of a 0.1% solution of FB (Polysciences Inc., Warrington, PA) was infused into the spinal cord over 2 minutes. The tip was left *in situ* for an additional 30 seconds prior to removal. This procedure was completed 3 additional times at the same co-ordinates at C6, C7 and C8 resulting in a total infusion of 300 nl of FB. Muscle was sutured with Vicryl and skin with monofilament suture. All animals received post-surgical antibiotics (Ampicillin, 100mg/kg subcutaneously) and analgesia (Buprenorphine 0.05mg/kg subcutaneously) for 2 days post lesion. All animals recovered uneventfully. Two weeks after FB tracer injections mice were either prepared for LCM (n=6/genotype, see LCM methods), or transcardially perfused with 4% paraformaldehyde (4% PFA), post-fixed overnight at 4^0C and embedded in 10% gelatin for immunohistochemical processing (n=12 PyX, n= 6 sham *ngr1*$^{+/+}$ *crym*-GFP mice*;* and n=12 PyX, n=9 sham *ngr1*$^{-/-}$ *crym*-GFP mice). An investigator blinded to genotype completed all surgical procedures.

In vivo validation, cortical AAV infusion and PyX

P35 C57Bl/6J mice (n=60) were acquired from Jackson Laboratories and randomized into 6 experimental groups, sham vehicle (n=9), PyX vehicle (n=11), sham AAV-*Lppr1* (n=7), PyX AAV-*Lppr1* (n=15), sham AM095 (n=6), and PyX AM095 (n=10). All mice received injection of two viruses into their right cortical hemispheres; AAV-mCherry (for anatomical tracing of the CST) and either AAV-*V5* (control) or AAV-*Lppr1-V5*. Prior to surgery, viruses were mixed, such that the final concentration of each virus was $2.55x10^{13}$ viral particles/ml, and aliquoted to blind surgeon to treatment. At P42, mice received cortical infusion of AAV into motor cortex. AAV transduction of CSMNs was completed as previously described for anterograde BDA labeling of CSMNs (Cafferty et al., 2010). Briefly, burr holes were made over the sensorimotor cortex and 5 micro infusions of 150 nl of a 1:1 viral mixture were made to a depth of 0.7 mm (co-ordinates, +1 mm to -1 mm posterior to bregma and 0.5 - 1.5 mm lateral to bregma) using a pulled glass capillary tube attached to a Micro4 infusion device to deliver a total volume of 375 nl of each virus (750 nl total). Muscle was sutured with Vicryl and skin with monofilament suture. All animals received post-surgical antibiotics (Ampicillin, 100mg/kg subcutaneously) and analgesia (Buprenorphine 0.05mg/kg subcutaneously) for 2 days post lesion. All animals recovered uneventfully. Two weeks after cortical infusion, mice underwent either unilateral PyX (left side) or sham lesion, as described above. Four weeks post lesion, mice were

perfused with 4% PFA, brain and spinal cord dissected and post-fixed overnight at 4^0C and embedded in 10% gelatin for immunohistochemical processing. An investigator blinded to treatment completed all surgical procedures.

Drug

AM095, a specific LPAR1 antagonist was acquired from Med Chem Express. A 3 mg/ml suspension of AM095 was made in 1% DMSO in sterile saline. Mice were given drug (30 mg/kg) or vehicle treatment via oral gavage every 12 hours for 10 days starting ~5 hours post PyX or sham lesion.

Behavioral analysis

Experimental mice used for *in vivo* validation of targets were assessed for skilled motor function using the grid walking task (Starkey et al., 2005). Mice were placed on an elevated 45 x 45 cm metal grid with 2.5 x 2.5 cm squares with dark cardboard walls creating a perimeter to make the environment more comfortable for the animals. Mice were videotaped via reflection from an angled mirror placed under the grid. Mice were recorded and allowed to explore the grid for 3 minutes. An experimenter blinded to treatment and lesion scored videos for the percentage of impaired steps out of the first 50 steps taken for each limb. Impaired steps included a foot slip where the limb fell completely between the rungs or an incorrectly placed step where either the ankle or the tips of the digits were placed on the rung instead of proper grasping of the rung. Animals were acclimated to the grid upon arrival from Jackson Labs, and then tested the day before AAV infusion, the day before PyX, and days 3, 7, 14, 21, and 28 post-lesion.

Histology

Mice were euthanized with CO_2 and were transcardially perfused with 0.9% NaCl (normal saline) followed by 4% PFA in PBS. Brains and spinal cords were dissected, post fixed in 4% PFA overnight at 4ºC and subsequently embedded in 10% gelatin (Sigma Aldrich) dissolved in water for vibratome sectioning. Transverse sections (35 µm) of cervical spinal cord (C6 - C7) and coronal sections of brain and brainstem were processed for *crym*-GFP or mCherry with tyramide signal amplification (Perkin Elmer, Waltham, MA). Immunofluorescence utilized primary antibodies directed against green fluorescent protein (GFP, 1:5000, Life Technologies, Grand Island, NY), mCherry (1:500, Abcam, USA), V5 (1:500, Sigma), and PKCgamma (1:400, Santa Cruz Biotechnology, USA) and detected with secondary antibodies Alexa Fluor-488, and -594 (1:500, Life Technologies, Grand Island, NY). An investigator blinded to treatment and lesion completed all immunohistochemical procedures.

Quantification

FB counts in cortex were made from brains cut coronally in 35 µm sections. An investigator blind to genotype and surgical treatment counted all FB+ cells in cortex from every fourth section on an epifluorescent microscope (Leica, DM5500) using a 10X objective. Data are presented as the average of the total number of FB+ cells counted per animal (n=6 sham *ngr1*$^{+/+}$ *crym*-GFP mice, n=6 sham *ngr1*$^{-/-}$ *crym*-GFP mice, n=6 PyX *ngr1*$^{+/+}$ *crym*-GFP mice, n=6 PyX *ngr1*$^{-/-}$ *crym*-GFP mice).

Transverse cervical spinal cord sections were cut from all experimental animals in candidate gene validation experiments to assess mCherry+ CST axon distribution. To determine the total number of CST axons labeled per animal, photomicrographs were taken at 63X (Zeiss Imager Z1) from three randomly selected sections from each animal. Low-power photomicrographs were taken at 10X to determine the area occupied by the CST in the ventral dorsal columns. A 25 x 25 µm grid was then overlaid on the 63X photomicrographs and the number of mCherry+ axons, in three randomly selected boxes from the grid, was counted. The average number of axons from these boxes was then scaled up to determine the total number of axons labeled. To determine the innervation density of mCherry+ axons into the ventral gray matter, an investigator blind to treatment and lesion took representative mosaic images of mCherry signal from 5 sections per animal C6-C8 using an epifluorescent microscope using a 10X objective. Using ImageJ, images underwent background subtraction using the rolling ball correction algorithm with a radius of 5 pixels and thresholding. Fiber length was then measured and normalized to the total number of CST axons counted in the dorsal columns. Analysis was conducted on the ventral horns of the intact and denervated spinal cords of all animals.

Laser Capture Microdissection (LCM), RNAseq and sequencing analysis

Four weeks after PyX and two weeks after FB tracing, *ngr1*$^{+/+}$ (n=6) and *ngr1*$^{-/-}$ (n=6) *crym*-GFP mice were sacrificed with an overdose of CO_2 and prepared for LCM. All procedures were done rapidly in order to minimize time between animal sacrifice and cell collection. Brains were rapidly dissected and snap frozen in isopentane on dry ice. Frozen brain was immediately transferred to cryostat (Leica Microsystems) set at -19ºC. Thin, 14 µm,

coronal sections through M1 cortex were cut and collected on PPS slides (Leica Microsystems). PPS slide membranes were pretreated with 30 minutes of UV exposure followed by 3 minutes treatment with sterile poly-D-lysine to sterilize and improve tissue adherence to the PPS membrane. After briefly allowing the sections to dry and adhere to the slide, slides were fixed in ice-cold acetone for 10 minutes. Slides were air dried for 1 minute and then immediately mounted for LCM by a LMD7000 equipped with epifluorescence (Leica Microsystems). The LMD7000 is equipped to collect multiple samples from the same specimen. Hence we were able to collect intact GFP+ non-sprouting CSMNs from the intact side, GFP+/FB+ (by switching between filters) intact sprouting CSMNs from the intact side, non-CST GFP- cortex from the intact side, and axotomized GFP+ CSMNs from the lesioned side all from the same specimen. This feature minimizes collection times and allows LCM of multiple different populations of cells from the same biological sample. Cells isolated via LCM were collected directly in RNA stabilizing buffer, RLT buffer (Qiagen) with 1% β-mercaptoethanol, and frozen. RNA was subsequently extracted using Qiagen RNeasy Micro Kit following the protocol for laser-captured cells. After purification, cells were pooled from two animals at random to obtain 3 replicates per condition from 6 animals per genotype for 21 total samples. Subsequent processing of RNA was completed in the collaboration with the Yale Center for Genome Analysis (YCGA).

Low-input RNA-seq sample preparation and sequencing

500 pg of total RNA was processed using the SMARTer Ultra Low kit (Clontech) according to the manufacturer's recommendations. Briefly, a proprietary oligo-dT based primer was used for first-strand synthesis followed by 12 cycles of amplification during second-strand synthesis. The resulting cDNA was sheared using focused acoustic sound waves (Covaris) to a mean size of approximately 140 base pairs. Magnetic AMPure XP beads (Beckman Coulter) was used to purify the cDNA and remained with the sample throughout sequencing library construction. Following each library process step, cDNA was selectively precipitated by weight and re-bound to the beads through the addition of a 20% polyethylene glycol, 2.5 M NaCl solution. T4 DNA polymerase and T4 polynucleotide kinase blunted ends and phosphorylated the fragments. The large Klenow fragment then added a single adenine residue to the 3' end of each fragment and custom adapters (from Integrated DNA Technology, IDT) were ligated using T4 DNA ligase. Adapter ligated fragments were then PCR amplified using custom-made primers (IDT). During PCR, a unique 6 base identifier was inserted at both ends of each DNA fragment to allow for multiplexing of samples during sequencing.

Sample concentrations were normalized to 2 nM and loaded onto Illumina rapid run flow cells at a concentration that yields 160-180 million passing filter clusters per lane. The samples were clustered on-board the equipment and sequenced four per lane using 76 bp single-ended reads on an Illumina HiSeq 2500, according to Illumina protocols, generating between 27 and 39 million reads per sample (see Tables S1 and S2). A positive control (prepared bacteriophage Phi X library) provided by Illumina was spiked into every lane at a concentration of 0.3% to monitor sequencing quality in real time.

Sequencing data analysis

Adapter sequences, empty reads, and low-quality sequences were removed; and the first 6 base pairs and the last 21 base pairs were trimmed to remove low quality bases using the FASTX tool kit (http://hannonlab.cshl.edu/fastx_toolkit.index.html). Trimmed reads were aligned using Tophat v.2.0.8 (Trapnell et al., 2009) to the latest reference UCSC mouse genome and transcript annotation (mm10) using the very sensitive alignment process. Only the reads that mapped to a single unique location within the genome, with a maximum of two mismatches in the anchor region of the spliced alignment, were reported. Default settings were used for all other Tophat settings. Tophat alignments were then processed by Cufflinks v2.1.1 (Trapnell et al., 2010) to obtain differential gene expression. Cufflinks software normalizes the read counts per gene, taking into account the effects of sequence depth and transcript length (reported as FPKMs, fragments per kilobase of transcript per million mapped reads), and perform statistical analysis to identify differentially expressed genes. Multiple testing between all samples using the Benjamini-Hochberg correction was used to determine significantly differentially expressed (SDE) genes (adjusted P value <0.05)(Trapnell et al., 2012). Recent versions of Cufflinks also incorporate a method for detection and correction of sequence-specific bias that challenges the assumption of uniform coverage, such as the bias caused by the use of random hexamers during library preparation. Following the standards proposed by the ENCODE project, samples were multiplexed to warranty a minimum of 20 million reads mapped to known genes per sample.

Differential gene expression analysis

To search for biological significance in our SDE gene list, network and pathway mapping was performed in Ingenuity Pathway analysis (IPA, QIAGEN Redwood City, CA, USA). SDE genes from Cufflinks were imported to IPA and a 'core analysis' was completed with the following cutoffs applied: log2fold change >1.5 and corrected *p*-value < 0.05. Fishers exact test *p*-value was used to determine the probability that the observed and predicted regulated gene sets overlap by chance. Unsupervised hierarchical clustering of SDE genes was completed in GENE E (Bioconductor, Broad Institute) using average linkage and one minus Pearson's correlation. Heat maps were constructed after normalizing FPKMs per gene.

AAV production

AAVs were generated in house to overexpress candidate genes to test for a functional role in enhancing sprouting *in vitro* and *in vivo*.

Plasmid preparation

AAV-mCherry construct was provided by Dr. In-Jung Kim (Yale University). This construct expresses mCherry under the CAG promoter followed by a WPRE enhancer and SV40 polyadenylation signal (Figure 5A). To generate AAV-CAG-mCherry, Dr. Kim modified two AAV vectors (Addgene plasmid #18917 and #38044). DNA of #18917 was cut with BamHI and Eco RI, vector backbone was kept and ligated with mCherry insert. mCherry sequence was amplified by PCR using the DNA of #38044 as a template with BamHI and EcoRI at the end of the amplified product for ligation.

To develop overexpression constructs, mCherry was replaced with YFP or the coding sequence of candidate genes. YFP was PCR amplified (forward primer: CGGGATCCACCATGGTGAGCAAGGGCGAGGA, reverse primer: GCGAATTCTTACTTGTACAGCTCGTCCA) from pEYFP-N1 (Clontech) and cut with EcoRI and BamHI. To remove mCherry, AAV-mCherry was cut with EcoRI and BamHI and ligated with cut YFP fragment to generate AAV-CAG-YFP. For candidate genes, primers to *Lppr1* (forward primer: GCACCGGTGAATTCCACCATGGCTGTAGAAAACAACAC, reverse primer: CGACCGGT GGTGACTTCGGTCATGGAGG) and *Inpp5k* (forward primer: CGACCGGTCCACCATGCAGCACGGAGACAGGAA, reverse primer: GCACCGGTGATCTGTGGCTCAGGCTCAT) were made using coding sequences available from NCBI (*Lppr1* gene ID: 272031, *Inpp5k* gene ID: 19062), with forward primers adding a Kozak sequence and AgeI site and reverse primers adding an AgeI site and removing the stop codon of the candidate gene. Candidate genes *Lppr1* and *Inpp5k* were PCR amplified using Platinum Pfx DNA polymerase (Thermo Scientific) from P1 brain cDNA library obtained from Dr. In-Jung Kim. Insertion of candidate genes was completed with several steps: removal of mCherry, insertion of V5, and insertion of candidate genes. mCherry was cut out of the AAV plasmid using BamHI and EcoRI, vector backbone, purified, and blunt cut (Qiagen quick blunting kit) to generate a blunted AAV vector. V5 was PCR amplified from a plasmid provided by Dr. Sourav Ghosh (Yale University) (forward primer: CGGATATCACCGGTGGTAAGCCTATCCCTAAC, reverse primer: CGGATATCTCACGTAGAATCGAGACCGAG) with the forward primer containing an EcoRV and AgeI site and the reverse primer containing an EcoRV site and stop codon for V5. V5 was cut with EcoRV and ligated to blunted AAV vector. AAV-*V5* and PCR amplified candidate genes were then cut with AgeI and ligated together to generate AAV-CAG-*Lppr1-V5* and AAV-CAG-*Inpp5k-V5*. Candidate gene TAZ was PCR amplified (forward primer: CGACCGGTCCACCATGGCCTACCCATACGATGT, reverse primer: GCACCGGTTTACAGCCAGGTTAGAAAGG) from an HA-TAZ plasmid that was a gift from Kunliang Guan (Addgene plasmid #32839) (Lei et al., 2008). The forward primer amplifying TAZ included the HA tag from the original plasmid to produce TAZ tagged with HA on the N-terminus. Amplified TAZ was cut with AgeI and blunted for ligation into the blunted AAV vector to generate AAV-CAG-HA-TAZ. An empty AAV vector containing just the V5 tag with its own start and stop codon in place of a gene, AAV-V5, was synthesized as a control by using the same procedure as above but with a modified forward primer (CGACCGGTCCACCATGGGTAAGCCTATCCCTAAC) that contained a Kozak sequence and start codon for V5. After tagged gene insertion, all plasmids were sequenced (Yale Keck Sequencing Facility) to verify correct coding sequence and ITR placement in the AAV vector. AAV plasmids expressing candidate genes or reporters were used for electroporation into acute dissociated neuronal cultures or for AAV synthesis.

AAV synthesis

For AAV production, a triple-transduction method was used as has been described previously (Park et al., 2015). Briefly, HEK 293 cells were cultured in ten 15 cm plates and polyethylenimine (Polysciences) transfected with an AAV plasmid overexpressing a candidate gene, delta F6 helper plasmid (UPenn Vector Core), and a plasmid

expressing AAV capsid 2/1 (UPenn Vector Core). Cells were harvested, pelleted, and resuspended in freezing buffer (0.15 M NaCl and 50 mM Tris, pH 8.0) 48-60 hours after transfection. For viral purification, cells were lysed by undergoing two freeze-thaw cycles followed by benzonase treatment (EMD Chemical) for 30 minutes at 37ºC. Lysate supernatant was collected by spinning tubes in a swinging bucket rotor (Eppendorf) at 3700g for 20 minutes. Lysate supernatant was then added dropwise to the top of a centrifuge tube containing a 15%, 25%, 40% and 60% iodixanol step gradient. The gradient was spun in a Vti50 rotor (Beckman Coulter) at 50,000 rpm for 2 hours at 10ºC. The 40% fraction was collected and added to an Amicon Ultracel 100K (Millipore) for buffer exchange to PBS. A small amount of virus was used to test viral titer using qPCR. Concentration of virus was repeated on smaller Amicon Ultracels (Millipore) until desired high titer was reached. Final purified virus was aliquoted and stored at -80ºC. To test the efficacy and efficiency of custom made AAVs, reporter AAV-YFP and AAV-mCherry were generated and purified. AAV-YFP and AAV-mCherry plasmids were singly or co-transduced into cortical neurons *in vitro* to determine transfection efficiency in culture. In neuronal culture with double transfection, 78% of neurons were transduced to express a reporter and 97% of infected cells expressed both reporters. To test AAV efficacy *in vivo*, AAV-YFP and AAV-mCherry were co-injected into cortex following the same procedure as described above for cortical BDA and AAV infusion. Three weeks post-transduction, animals were sacrificed, and tissue was fixed with 4% PFA for histology. >92% of cells in infusion site were infected with and expressing both reporters.

Cortical neuron culture

Embryonic cortical neurons were cultured as described previously (Zou et al., 2015). Briefly, E17 mouse embryos were dissected from timed-pregnant C57Bl/6 mice and cortices were rapidly dissected in ice-cold Hibernate E medium (Brain Bits). Cortices were then digested for 30 minutes at 37ºC using a digestion medium containing papain (25 U/ml, Worthington Biochemical), DNAse I (2000 U/ml, Roche), 2.5 mM EDTA, and 1.5 mM $CaCl_2$ in a neuronal culture medium composed of Neurobasal A (Life Technologies) with B27 supplement (Life Technologies), 1% sodium pyruvate (Life Technologies), 1% glutamax (Life Technologies), and 1% penstrep (Life Technologies). After digestion, cortices were washed twice with the neuronal culture medium and triturated in 2 ml of medium. Triturated cells were passed through a 40 µm cell strainer (Corning) and counted.

Acute dissociated cultures for outgrowth assay

Dissociated cortical neurons were electroporated with AAV plasmid to overexpress a candidate gene or reporter control (either YFP or mCherry). Dissociated cortical neurons were added to 100µl of Nucleofector solution (Lonza) and 3µg plasmid DNA. Cell mixture was transferred to a cuvette and electroporated in a Lonza Nucleofector 2b device using the device's pre-loaded mouse hippocampal neuron electroporation parameters. Electroporated neurons were then transferred to pre-warmed neuronal media and plated at a density of 2,000 cells per well in an 8-well glass Lab-Tek slide (Thermo Scientific) or 96-well plate pre-coated with poly-D-lysine (Corning) and laminin (Life Sciences). Neurons were placed in a 37ºC incubator for 72 hours and then fixed with 4% PFA in 4% sucrose. Neurons were visualized by staining for βIII-tubulin (1:2000, Promega) and DAPI (0.2mg/ml, Sigma). Electroporated neurons were identified by visualizing the control mCherry or YFP reporter or by staining for the V5 (1:1000, Sigma) or HA (1:1000, Sigma) tag on the candidate genes. For neuronal outgrowth assay, 96-well plates were imaged using a 10X objective on an ImageXpress Micro XLS (Molecular Devices). For each well, 4 locations were imaged and neuronal outgrowth was measured using the MetaXpress software for neuronal outgrowth (Molecular Devices). The software measured total neuronal outgrowth per cell, the number of processes off of the soma, and the number of branches per process. Data are presented as the average for each of these metrics over images from 4 locations per well from a minimum of 60 wells per condition from neuronal cultures obtained from 3 separate litters. For neurons plated on Lab-Tek slides, neurons were cultured for 3 days or 7 days at 37ºC before fixation with 4% PFA in 4% sucrose. Neurons were stained for βIII-tubulin (1:2000, Promega), DAPI (Vector Labs), Phalloidin (Life Sciences), and V5 or HA. Slides were visualized using an epifluorescent microscope (Leica Microsystems) for qualitative analysis of cellular morphology and candidate gene localization.

Scrape assay

Cells were plated on 96-well plates pre-coated with poly-D-lysine (Corning) at a density of 50,000 cells per well in 200 µl neuronal culture medium as described previously (Zou et al., 2015). Immediately after plating, 1 µl of AAV was applied to each well at a titer of $1.0x10^{10}$ viral particles/ml. Each plate contained wells that are given control AAV-YFP or AAV-mCherry virus to serve as a viral overexpression control for wells given AAVs to overexpress candidate genes. Neurons were then incubated at 37ºC. On DIV 7 and 14, 100 µl of medium was removed from each well and replaced with 100 µl fresh neuronal culture medium. Prior to medium exchange on DIV 14, 96-well

cultures were scraped using a custom-fabricated 96-pin array as described previously (Huebner et al., 2011, Zou et al., 2015). Neurons were placed back at 37ºC and allowed to regenerate for 72 hours before fixation with 4% PFA in 4% sucrose. Regenerating axons were then visualized by staining for βIII-tubulin (1:2000, Promega). Cell density was visualized using nuclear marker DAPI (0.2mg/ml, Sigma) to ensure that each well contained the same number of neurons after viral treatment. Images of the center of each well were taken using a 10X objective on an ImageXpress Micro XLS (Molecular Devices). The scrape zone was then analyzed for the total length of axons regenerating into the scrape zone in ImageJ by an investigator blind to treatment conditions. For each well, the total axon length of regenerating axons into the scrape zone was normalized to the average the total axon length of regenerating axon from control wells on that individual plate to create a regeneration index. Data presented is the average regeneration index of all wells (minimum 27 wells/condition) from cultures obtained from 3 separate litters.

Immunoblotting

Cortical neuron cultures were grown in 12-well PDL-coated plates. At 7 DIV, cells were lysed with RIPA buffer to collect total cell protein and subsequently sonicated at 15% every 0.5 seconds for 30 seconds. Protein was also collected from mice that received cortical infusion of AAV-*Lppr1-V5* or AAV-*V5* control into the right cortex (Figure S5I). Briefly, mice were euthanized two weeks after AAV infusion using CO_2 and were transcardially perfused with 0.9% NaCl (normal saline) for 2 minutes. Cortex ipsilateral and contralateral to AAV infusion was microdissected and immediately weighed and frozen on dry ice. Tissue was homogenized in RIPA buffer using a POLYTRON (Kinematica) and subsequently sonicated at 15% every 0.5 seconds for 30 seconds. Protein concentration was determined by Bradford assay (Bio-Rad Protein Assay) prior to dilution with Laemmli buffer (Bio-Rad). Samples were boiled at 95ºC for 5 minutes immediately before loading into a precast 4-20% tris-glycine gel (Bio-Rad). For culture lysates, 10 µg of protein was loaded per lane. For tissue lysates, 50 µg of protein was loaded per lane. Gels were transferred to activated PVDF membrane (Bio-Rad) using Trans-Blot Turbo transfer device (Bio-Rad) using the high-molecular weight transfer program. Membranes were blocked (Blocking Buffer for Fluorescent Western Blotting, Rockland) for 1 hour at room temperature on a rotating platform and incubated overnight with primary antibodies. Every membrane was stained for β-actin (1:2000, Cell Signaling) for a loading control and either V5 (1:1000, Sigma) or HA (1:1000, Sigma) to detect overexpression of LPPR1, INPP5K, or TAZ. Secondary antibodies were added for 2 hours (anti-mouse or anti-rabbit Alexa 488 or 546, Invitrogen) and proteins were visualized using Chemi-Doc MP imaging system (Bio-Rad).

SUPPLEMENTAL REFERENCES

ARLOTTA, P., MOLYNEAUX, B. J., CHEN, J., INOUE, J., KOMINAMI, R. & MACKLIS, J. D. 2005. Neuronal subtype-specific genes that control corticospinal motor neuron development in vivo. *Neuron,* 45**,** 207-21.

CAFFERTY, W. B., DUFFY, P., HUEBNER, E. & STRITTMATTER, S. M. 2010. MAG and OMgp synergize with Nogo-A to restrict axonal growth and neurological recovery after spinal cord trauma. *J Neurosci,* 30**,** 6825-37.

HUEBNER, E. A., KIM, B. G., DUFFY, P. J., BROWN, R. H. & STRITTMATTER, S. M. 2011. A multi-domain fragment of Nogo-A protein is a potent inhibitor of cortical axon regeneration via Nogo receptor 1. *J Biol Chem,* 286**,** 18026-36.

LEI, Q. Y., ZHANG, H., ZHAO, B., ZHA, Z. Y., BAI, F., PEI, X. H., ZHAO, S., XIONG, Y. & GUAN, K. L. 2008. TAZ promotes cell proliferation and epithelial-mesenchymal transition and is inhibited by the hippo pathway. *Mol Cell Biol,* 28**,** 2426-36.

PARK, S. J., BORGHUIS, B. G., RAHMANI, P., ZENG, Q., KIM, I. J. & DEMB, J. B. 2015. Function and Circuitry of VIP+ Interneurons in the Mouse Retina. *J Neurosci,* 35**,** 10685-700.

SIGAL, Y. J., QUINTERO, O. A., CHENEY, R. E. & MORRIS, A. J. 2007. Cdc42 and ARP2/3-independent regulation of filopodia by an integral membrane lipid-phosphatase-related protein. *J Cell Sci,* 120**,** 340-52.

STARKEY, M. L., BARRITT, A. W., YIP, P. K., DAVIES, M., HAMERS, F. P., MCMAHON, S. B. & BRADBURY, E. J. 2005. Assessing behavioural function following a pyramidotomy lesion of the corticospinal tract in adult mice. *Exp Neurol,* 195**,** 524-39.

TRAPNELL, C., PACHTER, L. & SALZBERG, S. L. 2009. TopHat: discovering splice junctions with RNA-Seq. *Bioinformatics,* 25**,** 1105-11.

TRAPNELL, C., ROBERTS, A., GOFF, L., PERTEA, G., KIM, D., KELLEY, D. R., PIMENTEL, H., SALZBERG, S. L., RINN, J. L. & PACHTER, L. 2012. Differential gene and transcript expression analysis of RNA-seq experiments with TopHat and Cufflinks. *Nat Protoc,* 7**,** 562-78.

TRAPNELL, C., WILLIAMS, B. A., PERTEA, G., MORTAZAVI, A., KWAN, G., VAN BAREN, M. J., SALZBERG, S. L., WOLD, B. J. & PACHTER, L. 2010. Transcript assembly and quantification by RNA-Seq reveals unannotated transcripts and isoform switching during cell differentiation. *Nat Biotechnol,* 28**,** 511-5.

VELMANS, T., BATTEFELD, A., GEIST, B., FARRES, A. S., STRAUSS, U. & BRAUER, A. U. 2013. Plasticity-related gene 3 promotes neurite shaft protrusion. *BMC Neurosci,* 14**,** 36.

ZHANG, Y., CHEN, K., SLOAN, S. A., BENNETT, M. L., SCHOLZE, A. R., O'KEEFFE, S., PHATNANI, H. P., GUARNIERI, P., CANEDA, C., RUDERISCH, N., DENG, S., LIDDELOW, S. A., ZHANG, C., DANEMAN, R., MANIATIS, T., BARRES, B. A. & WU, J. Q. 2014. An RNA-sequencing transcriptome and splicing database of glia, neurons, and vascular cells of the cerebral cortex. *J Neurosci,* 34**,** 11929-47.

ZOU, Y., STAGI, M., WANG, X., YIGITKANLI, K., SIEGEL, C. S., NAKATSU, F., CAFFERTY, W. B. & STRITTMATTER, S. M. 2015. Gene-Silencing Screen for Mammalian Axon Regeneration Identifies Inpp5f (Sac2) as an Endogenous Suppressor of Repair after Spinal Cord Injury. *J Neurosci,* 35**,** 10429-39.